27th EPS Conference on Contr. Fusion and Plasma Phys. Budapest, 12-16 June 2000 ECA Vol. **24B** (2000) 69 -72

Electron Acceleration due to High Frequency Instabilities at Supernova Remnant Shocks

K G McClements,[1] M E Dieckmann,[2] S C Chapman,[3] R O Dendy[1] and L O'C Drury[4]

[1] *EURATOM/UKAEA Fusion Association, Culham Science Centre, Abingdon, OX14 3DB, UK*

[2] *Institute of Technology and Natural Science, Linköping University, Campus Norrköping, S–601 74 Norrköping, Sweden*

[3] *Space and Astrophysics Group, Department of Physics, University of Warwick, Coventry, CV4 7AL, UK*

[4] *Dublin Institute for Advanced Studies, 5 Merrion Square, Dublin 2, Ireland*

1. Introduction

Observations of synchrotron radiation across a wide range of wavelengths indicate that strong collisionless shocks bounding shell–type supernova remnants (SNRs) accelerate electrons to relativistic energies. While diffusive shock acceleration [1] provides an efficient means of generating highly energetic electrons from a mildly relativistic threshold, it is not yet clear how this threshold can be reached. In this paper we show that it is possible for electrons to be accelerated to the required threshold by electrostatic waves driven by shock–reflected protons [2].

2. Particle–in–cell code simulations

Reflected protons are known to exist in a "foot" region upstream of perpendicular shocks, with thickness of the order of the upstream ion Larmor radius. The reflected protons form two beams, propagating towards and away from the shock, perpendicular to $\mathbf{B}$ [3]. We use a particle–in–cell (PIC) code to simulate instabilities driven by such beams, with bulk protons and electrons having zero net drift in the simulation frame: time evolution in the simulation can then be interpreted as spatial variation in the shock foot. The proton beams are initially Maxwellian with thermal speed $\delta u_\perp = 3 \times 10^5\,\mathrm{ms}^{-1}$ (defined such that the temperature is $m_p \delta u_\perp^2$, where m_p is proton mass), and drift speeds $u_{b\perp} = 3.25 v_{e0}$, $3.5 v_{e0}$, $5 v_{e0}$, $6 v_{e0}$, where $v_{e0} = 3.75 \times 10^6\,\mathrm{ms}^{-1}$ is initial electron thermal speed. The beam density is one third of the electron density: this is consistent with hybrid simulations of shocks with Alvénic Mach numbers ranging up to 60. The electron plasma frequency $\omega_{pe}/2\pi$ and gyrofrequency $\Omega_e/2\pi$ are 10^5Hz and 10^4Hz respectively. Normalized variables $\tilde{t} = \Omega_e t/2\pi$ and $\tilde{k} = k v_{e0}/\Omega_e$ are used to measure time t and wavenumber k. The simulations have one space dimension (y), orthogonal to $\mathbf{B}$, and 350 grid cells.

In all four simulations energy was transferred from beam protons to electrons, but the power flux between the two species increased dramatically when $u_{b\perp}$ was raised from $3.5 v_{e0}$ to $5 v_{e0}$. Fig. 1 shows the time evolution of perpendicular kinetic energy and electric field energy for $u_{b\perp} = 6 v_{e0}$. The distributions in perpendicular speed $v_\perp$ at $\tilde{t} = 70$ in the simulations with $u_{b\perp} = 5 v_{e0}$ and $u_{b\perp} = 6 v_{e0}$ (Fig. 2) can both be approximated by single Maxwellians, respectively with $v_e \simeq 8 v_{e0}$ and $v_e \simeq 12 v_{e0}$: the perpendicular

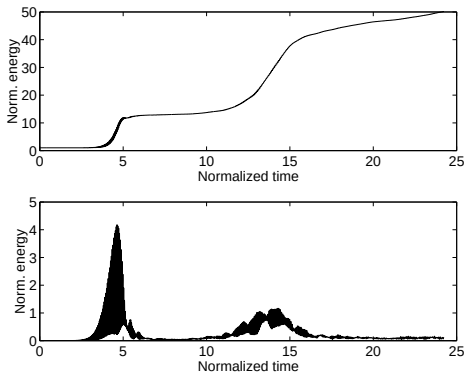

Fig. 1. *Electron perpendicular kinetic energy (upper) and electrostatic field energy (lower) versus $\tilde{t}$ for $u_{b\perp} = 6v_{e0}$.*

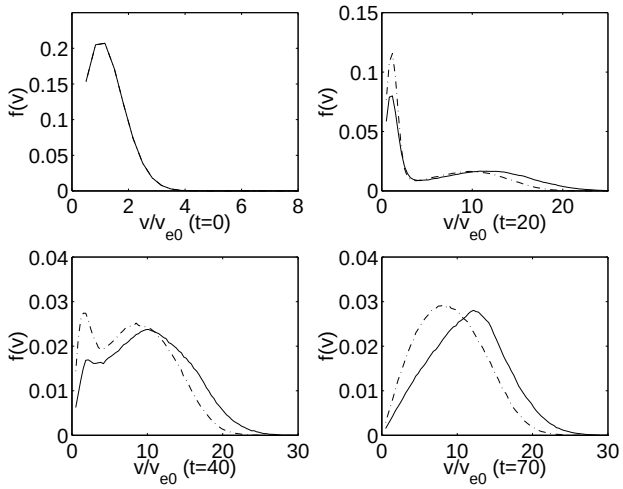

Fig. 2. *Electron perpendicular speed distributions for $u_{b\perp} = 5v_{e0}$ (dashed) and $u_{b\perp} = 6v_{e0}$ (solid).*

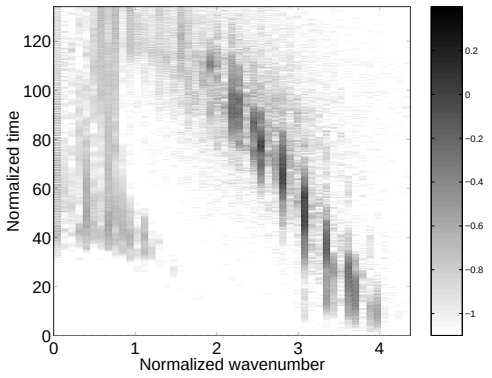

Fig. 3. *Electric field amplitude versus $\tilde{k}$ and $\tilde{t}$ when $u_{b\perp} = 3.25v_{e0}$.*

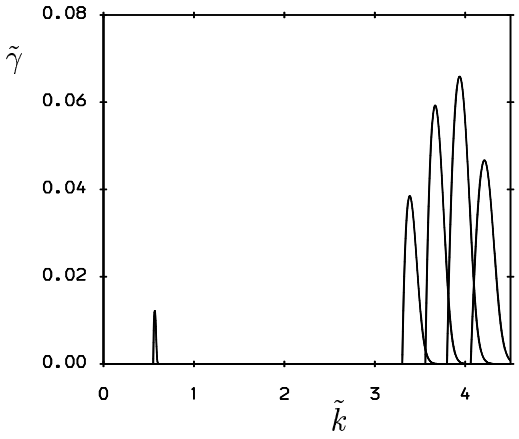

Fig. 4. *Growth rates of waves with $\omega > \Omega_e$ when $u_{b\perp} = 3.25v_{e0}$.*

thermal speeds thus exceed the velocities of the proton beams which produced them. In the case of $u_{b\perp} = 6v_{e0}$, the final electron temperature (11.5 keV) is easily sufficient to account for thermal X–ray emission observed from SNRs such as Cas A [4]. Individual electron energies of up to several tens of keV were observed in this simulation.

Fig. 3 shows the time evolution of wave amplitude versus $\tilde{k}$ when $u_{b\perp} = 3.25v_{e0}$. Instability occurs at discrete, regularly–spaced wavenumbers clustered around $\tilde{k} \simeq 3 - 4$. Fig. 4 shows $\tilde{\gamma}$, the growth rate normalized to Ω_e, obtained by solving the electrostatic dispersion relation

$$1 - \frac{\omega_{pi}^2}{\omega^2} + \frac{2\omega_{pb}^2\left[1 + \zeta_b Z(\zeta_b)\right]}{k^2\delta u_\perp^2} - \frac{\omega_{pe}^2}{\omega}\frac{e^{-\lambda_e}}{\lambda_e}\sum_{\ell=-\infty}^{\infty}\frac{\ell^2 I_\ell}{\omega - \ell\Omega_e} = 0\,, \qquad (1)$$

for the initial parameters of the simulation. In Eq. (1) ω_{pi}, ω_{pb} are background and beam proton plasma frequencies, Z is the plasma dispersion function with argument $\zeta_b \equiv (\omega - ku_{b\perp})/k\delta u_\perp$, and I_ℓ is the modified Bessel function of the first kind of order ℓ

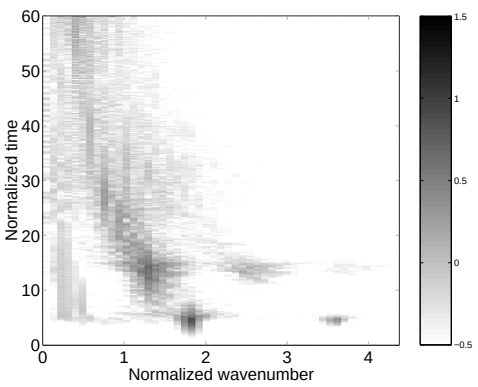

Fig. 5. *Electric field amplitude versus* $\tilde{k}$ *and* $\tilde{t}$ *when* $u_{b\perp} = 6v_{e0}$.

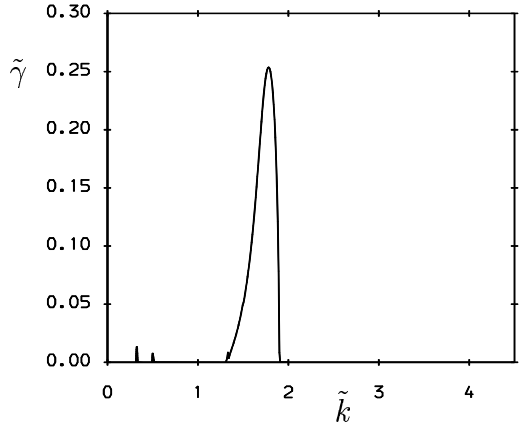

Fig. 6. *Growth rates of waves with* $\omega > \Omega_e$ *when* $u_{b\perp} = 6v_{e0}$.

with argument $\lambda_e \equiv v_{e0}^2 k^2/\Omega_e^2$. The most unstable waves have frequencies $\omega \simeq \omega_{pe}$, but are essentially cyclotronic: they can be identified as electron Bernstein modes. Figs. 5 and 6 show corresponding results for the simulation with $u_{b\perp} = 6v_{e0}$. Waves with $\tilde{k} \simeq 1.8$ rise sharply in magnitude at $\tilde{t} \simeq 3$, reaching a peak electric field amplitude $E = 35\,\mathrm{Vm}^{-1}$ and generating a harmonic at $\tilde{k} \simeq 3.6$. As in the simulation with $u_{b\perp} = 3.25v_{e0}$, the most unstable waves have $\omega \simeq \omega_{pe}$, but in this case they are unaffected by the magnetic field: the growth rate does not depend on the proximity of ω to cyclotron harmonics. After $\tilde{t} \simeq 8$, when the initial wave activity has ceased, a more broadband perturbation is generated at $\tilde{k} \simeq 1.3$, the mean $\tilde{k}$ decreasing with time.

3. Interpretation

The mode appearing early in the simulation with $u_{b\perp} = 6v_{e0}$ arises from a Buneman instability driven by beam protons. If $\omega_{pe}/\Omega_e \gg 1$, and the instability drive is sufficiently strong, electrons are effectively unmagnetized and, in the frame used in the simulations, the mode has frequency $\omega \simeq k u_{b\perp} \simeq \omega_{pe}$ and growth rate $\gamma \simeq (3\sqrt{3}\omega_{pb}^2\omega_{pe}/16)^{1/3}$ [2]. Solving the dispersion relation for unmagnetized electrons and $u_{b\perp} = 6v_{e0}$, we obtain results which are almost identical to those obtained in the magnetized case [Eq. (1)]. Even for $u_{b\perp} = 3.25v_{e0}$ the unmagnetized dispersion relation yields instability at about the same k and ω as Eq. (1), although the growth rates are somewhat lower. The essential difference between the simulations with $u_{b\perp} = 3.25v_{e0}$ and $u_{b\perp} = 6v_{e0}$ is that γ in the former case is too small for the electron gyromotion to be neglected: the instability is thus modified by cyclotronic effects, although it remains Buneman–like in character.

In every simulation wave excitation is correlated with acceleration and heating of electrons. Although particles can be energized via Landau damping, one would expect this process to be of limited effectiveness when, as in the present case, the waves are propagating perpendicular to a magnetic field. It is likely therefore that the strong acceleration observed in the simulations is due at least in part to nonlinear processes. The interaction of a large amplitude electrostatic wave propagating in the y direction with a particle of mass m and gyrofrequency Ω is described by a Hamiltonian [5]

$$h = \frac{1}{2}(p_x + y)^2 + \frac{1}{2}{p_y}^2 - \alpha \sin(y - \tilde{\omega}t), \qquad (2)$$

where y is normalized to $1/k$, canonical momentum components p_x, p_y are normalized to $m\Omega/k$, $\tilde{\omega} = \omega/\Omega$, and $\alpha \equiv (E/B)/(\Omega/k)$ determines the extent to which the system phase space is stochastic. Karney [5] solved the canonical equations corresponding to Eq. (2) for a range of conditions, plotting normalized Larmor radius $r = kv_\perp/\Omega$ versus wave phase angle ϕ at the particle's position, for successive transits through a particular gyrophase angle. For small α, all particles have regular orbits, represented by smooth curves $r = r(\phi)$ spanning all ϕ. When α exceeds a certain threshold, islands appear in (r, ϕ) space. Further increases in α cause stochasticity and hence particle acceleration. The analysis in [5] implies a critical electric field for island formation [2]:

$$E_i = \frac{v_\perp B|\tilde{\omega} - \ell|}{\ell|\frac{\ell}{r}J_\ell(r) - J_{\ell+1}(r)|}, \tag{3}$$

where J_ℓ is the Bessel function of order ℓ, $\ell\Omega$ being the cyclotron harmonic which ω is closest to. When $u_{b\perp} = 5v_{e0}$, $6v_{e0}$ wave growth occurs across a range of frequencies which includes cyclotron harmonics: in such cases $\tilde{\omega} = \ell$, and any finite wave amplitude will cause islands to be formed. This implies strong stochasticity and hence rapid electron acceleration (cf. Figs. 1–2). When $u_{b\perp} = 3.25v_{e0}$, $3.5v_{e0}$, on the other hand, the unstable frequencies lie between cyclotron harmonics, and E_i is finite. The maximum values of E in these simulations are only slightly higher than E_i, and one would then expect little stochasticity to occur.

4. Conclusions

Using PIC simulations and analytical theory we have shown that electrostatic waves in the ω_{pe} range, excited by protons reflected from high Mach number perpendicular shocks, can effectively heat and accelerate electrons. This process may help to account for observations of thermal bremsstrahlung from supernova remnants, and could also provide a seed population for diffusive shock acceleration to GeV energies. Our results confirm an earlier suggestion [4] that streaming between reflected protons and upstream electrons gives rise to a strong Buneman instability. The geometry used in the PIC simulations excludes the possibility of acceleration along $\mathbf{B}$, for example via the modified two–stream instability [3]. It is likely that the Buneman instability and the modified two–stream instability both play important roles in the production of high energy electrons at SNRs.

This work was supported by the CEC under TMR Contract ERB–CHRXCT980168, the UK Dept. of Trade & Industry, and EURATOM. S. C. Chapman was supported by a PPARC lecturer fellowship.

[1] A R Bell, Mon. Not. R. Astron. Soc. **182**, 147 (1978)

[2] M E Dieckmann et al., Astron. Astrophys. **356**, 377 (2000)

[3] K G McClements et al., Mon. Not. R. Astron. Soc. **291**, 241 (1997)

[4] K Papadopoulos, Astrophys. Space Sci. **144**, 535 (1988)

[5] C F F Karney, Phys. Fluids **21**, 1584 (1978)